Impact of Superficial Gas Velocity on Gas Holdup in a Cu-Cl Cycle Thermochemical Oxygen Bubble Column Reactor

M. W. Abdulrahman[1], N. Nassar[1]
[1]Rochester Institute of Technology (RIT), Department of Mechanical and Industrial Engineering
Dubai Silicon Oasis, Dubai, UAE
mwacad@rit.edu; nin8507@g.rit.edu

Abstract - *The necessity to investigate a variety of hydrogen production technologies has been prompted by the increasing popularity of hydrogen as an alternative fuel. This investigation investigates the hydrodynamics of the specific substances utilized in the oxygen generation reactor, specifically molten CuCl and oxygen gas, in the context of hydrogen production through the copper-chlorine (Cu-Cl) cycle. In order to accomplish this, a three-dimensional Eulerian-Eulerian Computational Fluid Dynamics (CFD) model is implemented. The primary objective of the study is to verify the precision of material simulations that were conducted in a previous investigation for the oxygen reactor. Helium gas at 90°C and liquid water at 20°C were employed in that investigation to simulate the hydrodynamic behaviour of the actual materials. The three-dimensional O_2-CuCl CFD model effectively simulates variations in gas holdup that occur as a result of changes in superficial gas velocity, with a maximum error of 29.9%. This error is the result of the complexity of the 3D multiphase system and the cumulative percentage errors associated with the hydrodynamic dimensionless parameters used in the previous material substitutions. Furthermore, the model shows that the gas holdup values of the actual materials are generally underestimated in comparison to those of the simulated materials.*

Keywords: Cu-Cl cycle, 3D CFD, gas holdup, superficial gas velocity, hydrogen production.

1. Introduction

It is anticipated that hydrogen will be essential in the development of sustainable energy in the future, as it has the ability to considerably reduce greenhouse gas emissions and pollution. Although the production of hydrogen gas from a variety of fuel sources can lead to a small amount of greenhouse gas emissions, these emissions are significantly lower than those produced by petroleum and diesel vehicles. Thermochemical cycles, particularly when employed in conjunction with nuclear reactors, offer a promising method for the thermal decomposition of water into hydrogen and oxygen through various stages. The copper-chlorine (Cu-Cl) cycle, which Argonne National Laboratories (ANL) has identified as a promising low-temperature cycle, necessitates a high-temperature heat source for the oxygen reaction [1-2]. Non-polluting sources, such as solar thermal energy or nuclear reactors, can provide this heat. Heating the molten salt within the oxygen reactor is a practicable and efficient method for transferring heat from the molten CuCl to the solid Cu_2OCl_2 reactant particles. Numerous heat transfer mechanisms have been investigated for the oxygen reactor, with direct contact heat transfer from oxygen gas to molten CuCl being the most effective [3-8]. This method involves the direct transfer of heat to the molten salt by heating a portion of the oxygen gas generated during the reactor's decomposition process to 530°C and reintroducing it into the reactor.

The Cu-Cl cycle's oxygen generation stage is an endothermic process that necessitates a temperature of 530°C and 129.2 kJ/mol of reaction heat [9]. Consequently, in order to elevate and sustain the reactor's temperature, external heat must be supplied.

The most effective method for the oxygen reactor is direct contact heat transmission using a Bubble Column Reactor (BCR). Although bubble columns provide benefits in a variety of industrial applications, the scale-up, modelling, and design of these structures are difficult due to the necessity of a comprehensive understanding of kinetics, hydrodynamics, heat and mass transfer, and chemical reaction rates. Gas holdup is a dimensionless parameter that denotes the volume fraction of gas within the BCR and is a critical performance indicator for bubble columns [10]. The objective of this study is to numerically investigate the multiphase hydrodynamics of a direct contact heat transfer reactor, with a particular emphasis on the interaction between molten CuCl salt and oxygen gas bubbles in the oxygen reactor of the Cu-Cl cycle. This will be achieved through the use of 3D Computational Fluid Dynamics (CFD) simulations. Over the years, research on bubble column reactors has been conducted using both experimental techniques and numerical simulations. Li et al. [11] employed both experimental methods and Computational Fluid Dynamics (CFD) to conduct hydrodynamic investigations on an air-water-glass bead slurry bubble column. The reactor was simulated using a 2D axisymmetric two-fluid Euler k-ε model. Their findings indicated that the primary obstacle to scaling up bubble columns is the changes in hydrodynamic characteristics that occur as column diameters varied. The gas holdup remains virtually constant, while the axial liquid velocity in the column's core increases significantly in columns with larger diameters. Additionally, they noted an increase in turbulent kinetic energy as the column size was increased. Sarhan et al. [12] employed a 3D CFD model and the population balance equation to examine the impact of the physical and chemical properties of the liquid and gas phases on bubble formation and hydrodynamics in a bubble column reactor. They utilized a Euler-Euler CFD model to closely approximate the experimental results of gas holdup under various phase flow conditions, achieving an accuracy of ±7%. Additionally, their investigation disclosed a minor rise in gas holdup as the density of the gas phase increased.

In a three-phase system composed of air, water, and glass particulate, Li and Zhong [13] employed a Eulerian-Eulerian-Eulerian approach to conduct a three-dimensional, time-dependent Computational Fluid Dynamics (CFD) analysis of three distinct bubble column reactors. They examined the hydrodynamics in relation to the time step, momentum discretization schemes, and wall boundary conditions. The reactors they modelled

were based on Gandhi et al. (height: 2500 mm, static height: 1500 mm, diameter: 150 mm), Rapure et al. (height: 2000 mm, static height: 1000 mm, diameter: 200 mm), and their own model (height: 800 mm, width: 100 mm, depth: 10 mm). The simulations were conducted using the RNG k-ε turbulence model. The optimal conditions for aligning with experimental data were determined by their findings, which included the use of a no-slip boundary condition, momentum discretization with a second-order upwind scheme, and a time step of 0.001 seconds.

In order to investigate the hydrodynamics and direct heat transfer characteristics of a two-phase flow model (air-molten salt), Pu et al. [14] conducted a two-dimensional CFD simulation of a molten salt bubble column. They implemented a Euler-Euler multiphase model in conjunction with a k-ε turbulence model. The superficial gas velocity, static liquid heights, operational pressure, and inlet gas temperature were all adjusted during the simulation. The investigation demonstrated that the molten salt temperatures and the rate of temperature increase over time were both increased as a result of an increase in the superficial gas velocity or operational pressure. Conversely, the rate of temperature increase was decelerated as the static liquid height increased. Furthermore, the volumetric heat transfer coefficient was improved by an increase in superficial gas velocity or operating pressure, whereas it was decreased by an increase in static liquid height.

In order to examine the distribution of local gas-liquid slip velocities in a bubble column, Zhang and Luo [15] created a two-phase (air-water) CFD model. Their focus was on the correlation between these velocities and heat transfer in a heterogeneous regime. Their research also examined the average variations in slip velocities over time as superficial gas velocities, axial positions, and bubble column sizes were altered. They employed a RNG k-ε turbulence model to conduct CFD-PBM (population balance model) simulations. The results suggested that the local gas-liquid slip velocities in the fully developed flow regions were elevated as a result of the increased superficial gas velocities. The slip velocities were more significantly influenced by radial position within the column at higher superficial gas velocities, with lower velocities near the centre compared to the fully developed flow regions. In these completely developed regions, the velocities of slip were minimally influenced by the height along the axis.

Using a 2D CFD PBM model, Li et al. [16] investigated the impact of a circular heat exchanger on

the hydrodynamics of a pilot-scale slurry bubble column reactor. For their simulations, they employed a RNG k-ε turbulence model in conjunction with a Euler-Euler multiphase model. A circular heat exchanger, which measured 108 cm in height, was installed in the reactor, which had a diameter of 30 cm and a height of 200 cm. Paraffin oil and catalyst particles were implemented in the simulations. The study determined that the gas phase was prominently distributed, and the circular heat exchanger tube's presence resulted in the formation of local circular vortices and robust slurry circulation. The bimodal profile of gas holdup in the radial direction was the result of the circular gas distributor's specific layout. Furthermore, the circular heat exchanger tube amplified this distribution, which led to a greater gas holdup and improved momentum transfer.

Zhou et al. [17] developed a conceptual model known as the particle-dependent dual bubble size (PDBS) model to examine the impact of particles on gas-liquid fluxes in a slurry bubble column. This model investigated the impact of particle addition on the bubble drag coefficient and the effects of variations in viscosity and density when particles are present. The research employed a three-phase system consisting of glass beads, water, and oxygen. It was determined that the stability of the slurry was enhanced by an increase in density and viscosity, as demonstrated by a delayed transition to a higher flow regime. The study determined that the gas holdup was diminished by increased solid concentrations in the slurry.

In order to examine the flow dynamics of syngas in a three-phase system (syngas, paraffin oil, solid particulates), Wodolazski [18] performed a 3D CFD simulation of a slurry bubble column reactor. The study employed a k-ε turbulence model with a Eulerian-Eulerian approach, with an emphasis on parameters including superficial gas velocity, initial solid particle concentration (ranging from 10% to 50%), gas holdup, and bubble size distribution. The results suggested that a reduction in axial gas holdup was the result of an increase in slurry concentration. Additionally, the rate of bubble breakup was diminished as a consequence of a higher slurry concentration. The study also observed an approximate parabolic relationship between the axial solid holdup profile and the effects of gas velocity. Matiazzo [19] conducted a thorough 3D computational fluid dynamics (CFD) investigation that concentrated on the complicated gas-liquid flow within a churn turbulent regime. The objective of the study was to assess the precision of a variety of models in predicting critical

factors, including drag closures, breakdown, and coalescence of bubbles.

Ertekin et al. [20] adjusted variables such as the superficial gas velocities, which ranged from 0.03 m/s to 0.25 m/s, and the column diameter, which ranged from 0.19 m to 3 m. In order to simulate the hydrodynamics of a high-pressure, air-water bubble column, Yan et al. [21] implemented three distinct optimized drag models. They examined the influence of varying reactor pressures (0.5, 1.0, 1.5, and 2.0 MPa) and superficial gas velocities (0.121, 0.174, 0.233, and 0.296 meters per second) on the radial gas holdup. The experimental data obtained through the electrical resistance tomography method was compared to the results of 2D and 3D CFD simulations.

A two-phase, gas-liquid, Eulerian-Eulerian, k-ε mixture turbulence CFD model was devised by Adam and Tuwaechi [22] to examine the impact of gas holdup and superficial gas velocity on the hydrodynamics. They noted that the volume fraction increased as the time step was increased. More detailed insights were obtained by employing a finer mesh with a grid resolution of 0.005. Pourtousi et al. [23] investigated the bubble column regime, with a particular emphasis on the impact of varying superficial gas velocities (0.0025 – 0.015 m/s) and bubble dimensions (3, 4, 5, and 5.5 mm) on the flow pattern predictions derived from Euler-Euler simulations. They developed a 3D air-water CFD simulation for a slurry bubble column with a diameter of 0.288 m and a height of 2.6 m.

Abdulrahman conducted dimensional analysis studies using the Buckingham pi theorem due to the difficulties associated with utilizing the actual materials of the oxygen production reactor (molten CuCl and O_2 gas) for laboratory experiments. In an effort to stimulate the actual materials of the oxygen production reactor with more appropriate materials that are safe for laboratory use, this analysis was conducted. He designated liquid water at 22°C and helium gas at 90°C as the simulated materials. Within a specific margin of error, these materials can replicate the behaviour of the actual materials in terms of heat transfer and hydrodynamics [24-25]. Abdulrahman has conducted 2D CFD simulations and experiments to examine the hydrodynamics of the slurry bubble column reactor, which involves direct contact heat transfer between the helium gas at 90°C and the slurry of water and alumina particulates at 20°C. The temperature distribution of the helium gas inside the slurry bubble column, as well as the volumetric heat transfer coefficient, transition velocity,

and gas holdup, were the parameters that he examined [8, 26-35]. Abdulrahman and Nassar conducted a review of the Eulerian approach for CFD analyses of bubble column reactors [36]. In addition, they have created a 3D CFD simulation for the oxygen production reactor, which is a slurry bubble column reactor that contains alumina solid particles, water liquid, and helium gas. Using simulated materials of liquid water and helium gas, they have examined the impact of solid concentration, static liquid height, and superficial gas velocity on gas holdup [37-40].

It is evident from a comprehensive examination of the existing literature that 3D computational fluid dynamics (CFD) simulations have not been conducted previously with the actual materials in the copper-chlorine (Cu-Cl) cycle, with a focus on the thermal hydraulics of oxygen bubble column reactors. Additionally, the oxygen bubble column rector has been the subject of previous CFD studies by Abdulrahman and Nassar [37-42], which have concentrated on simulated materials of helium gas and liquid water rather than the actual materials of molten CuCl and oxygen gas. The objective of this paper is to compare the results of the 3D CFD simulations of the actual materials of the oxygen production reactor in the Cu-Cl cycle of hydrogen production with those of the simulated materials in order to validate the material simulations developed by Abdulrahman [24-25].

2. Simulations of CFD
2.1. Governing Equations
In this investigation, computational fluid dynamics (CFD) simulations are conducted for a three-dimensional system in conjunction with a pressure-based solver, a Eulerian-Eulerian model, and a Eulerian sub-model. Table 1 illustrates the equations implemented during the computational fluid dynamics (CFD) analysis. These equations are exclusively designed for the gas phase. The equations for the liquid phase are not repeated for the sake of brevity, as they are comparable to those for the gas phase.

Table 1: Comprehensive overview of equations applied in 3D CFD simulations.

Description [reference]	Equation
Volume equation [43]	$V_g = \int_V \alpha_g \, dV$
Continuity equation in 3D Polar coordinates (r, θ, y) [8]	$\nabla . V_g = \frac{\partial v_{r,g}}{\partial r} + \frac{v_{r,g}}{r} + \frac{1}{r}\frac{\partial v_{\theta,g}}{\partial \theta} + \frac{\partial v_{y,g}}{\partial y} = 0$
Momentum equation in 3D Polar coordinates [8]	$\rho_g \alpha_g (\frac{\partial v_r}{\partial t} + v_r \frac{\partial v_r}{\partial r} + \frac{v_\theta}{r}\frac{\partial v_r}{\partial \theta} + vy\frac{\partial v_r}{\partial y} - \frac{v_\theta^2}{r}) = -\alpha_g \frac{\partial P}{\partial r} + \alpha_g \frac{\mu_{g,eff}}{3}\frac{\partial(\nabla.V)}{\partial r} + \mu_{g,eff}\,\alpha_g[\frac{1}{r}\frac{\partial}{\partial r}(r\frac{\partial v_r}{\partial r}) + \frac{1}{r^2}\frac{\partial^2 v_r}{\partial \theta^2} + \frac{\partial^2 v_r}{\partial y^2} - \frac{v_r}{r^2} - \frac{2}{r^2}\frac{\partial v_\theta}{\partial \theta}] + \rho_g \alpha_g\, g_r + M_{i,g,r}$ $\rho_g \alpha_g(\frac{\partial v_\theta}{\partial t} + v_r\frac{\partial v_\theta}{\partial r} + \frac{v_\theta}{r}\frac{\partial v_\theta}{\partial \theta} + v_y\frac{\partial v_\theta}{\partial y} + \frac{v_r v_\theta}{r}) = -\alpha_g\frac{1}{r}\frac{\partial P}{\partial \theta} + \alpha_g\frac{\mu_{g,eff}}{3r}\frac{\partial(\nabla.V)}{\partial \theta} + \alpha_g\mu_{g,eff}[\frac{1}{r}\frac{\partial}{\partial r}(r\frac{\partial v_\theta}{\partial r}) + \frac{1}{r^2}\frac{\partial^2 v_\theta}{\partial \theta^2} + \frac{\partial^2 v_\theta}{\partial y^2} + \frac{2}{r^2}\frac{\partial v_r}{\partial \theta} - \frac{v_\theta}{r^2}] + \rho_g \alpha_g\, g_\theta + M_{i,g,\theta}$ $\rho_g \alpha_g(\frac{\partial v_y}{\partial t} + v_r\frac{\partial v_y}{\partial r} + \frac{v_\theta}{r}\frac{\partial v_y}{\partial \theta} + v_y\frac{\partial v_y}{\partial y}) = -\alpha_g\frac{\partial P}{\partial y} + \alpha_g\,\mu_{g,eff}[\frac{1}{r}\frac{\partial}{\partial r}(r\frac{\partial v_y}{\partial r}) + \frac{1}{r^2}\frac{\partial^2 v_y}{\partial \theta^2} + \frac{\partial^2 v_y}{\partial y^2}] + \rho_g \alpha_g g_y + M_{i,g,y}$
Energy equation in 3D Polar coordinates [8]	$\alpha_g \rho_g C\,(\frac{\partial T_g}{\partial t} + v_{r,g}\frac{\partial T_g}{\partial r} + \frac{v_{\theta,g}}{r}\frac{\partial T_g}{\partial \theta} + v_{y,g}\frac{\partial T_g}{\partial y}) = \bar{\bar{\tau}}_g : \nabla V_g + k_g(\frac{1}{r}\frac{\partial}{\partial r}(r\frac{\partial T_g}{\partial r}) + \frac{1}{r^2}\frac{\partial^2 Tg}{\partial \theta^2} + \frac{\partial^2 T_g}{\partial y^2}) + S_g + Q_{g,sl}$
Effective density	$\hat{\rho}_g = \alpha_g\, \rho_g$
Drag force [43]	$M_D = \frac{\rho_g f}{6\,\tau_b}\, d_b\, A_i\, (\boldsymbol{V_g} - \boldsymbol{V_l})$
Interfacial area [43]	$A_i = \frac{6\,\alpha_g\,(1-\alpha_g)}{d_b}$
Schiller-Naumann drag equation [44]	$C_D = \begin{cases} \frac{24\,(1+0.15\,Re_b^{0.687})}{Re_b} & Re_b \le 1000 \\ 0.44 & Re_b > 1000 \end{cases}$

The reactor's design dimensions in this paper are derived from the Helium-Water bubble column reactor

investigated by Abdulrahman [26-28]. However, the material properties have been modified to correspond with those of oxygen and Cupreous Chloride. In accordance with Abdulrahman's property comparison [24-25], the Helium-Water (He-H_2O) and the O_2-CuCl systems are comparable. In order to guarantee comparability, the superficial gas velocity of the O_2-CuCl system is carefully adjusted to maintain the same Reynolds number as that of the He-H_2O system. The reactor employed in this investigation is cylindrical in form, with a diameter of 21.6 cm and a height of 91.5 cm. The gas is introduced into the bubble column reactor through a six-arm sparger-type gas distributor, each arm containing 12 orifices with a diameter of 0.3 cm, resulting in a total of 72 orifices.

The Reynolds-Averaged Navier-Stokes (RANS) models, including k-ε and k-ω, are the least computationally expensive methods for estimating complex turbulent flows, and they are the turbulence model used in this investigation. These models are capable of accurately simulating a wide range of turbulent flows and heat transfer processes. The RNG k-ε model is selected due to its greater accuracy and reliability across a broader spectrum of flows in comparison to the conventional k-ε model. This study emphasizes the suitability of this model for the simulation of churn turbulent flow. The dispersed turbulence model is the k-ε sub-model that was chosen as a result of the low gas phase concentrations and the significant variance in phase densities between liquid and gas. Furthermore, this turbulence model is computationally less expensive than the per-phase turbulence model. The application of the standard wall function to wall boundary conditions is a common practice in industries, as it yields reasonable results for a diverse array of wall-bounded flows.

For the Bubble Column Reactor (BCR), a hexahedron mesh is implemented, and mesh independence is implemented to guarantee that the maximum mesh size is chosen to minimize computational costs while achieving satisfactory performance. Using finer meshes results in a 3% difference in the gas holdup, as the final mesh consists of 26,825 nodes and 24,396 elements.

2.2. Boundary Conditions

The simulated BCR comprises three distinct boundaries, namely the wall boundary conditions and inlet and outlet boundary conditions. The inlet boundary condition is specified with gas at a uniform velocity and a volume fraction of 1. The gas velocity at the inlet (sparger) is defined as the volumetric flow rate of the gas at the inlet $(\dot{V}_{g,in})$ divided by the total cross-sectional area of the sparger (A).

$$v_g = \frac{\dot{V}_{g,in}}{A}$$

The superficial gas velocity U_{gs} is the gas velocity v_g multiplied by the gas volume fraction α_g.

$$U_{gs} = \alpha_g v_g$$

The superficial gas velocity at the inlet is equal to the gas velocity at the inlet because the volume fraction of the gas through the sparger is 1. From above, the boundary conditions at the inlet will be:

At $y = 0$, $\alpha_g = 1$ and $U_{gs} = \alpha_g v_g = v_g = \frac{\dot{V}_{g,in}}{A}$

The pressure is not specified at the inlet because of the incompressible gas phase assumption (relatively low pressure drop system). The pressure boundary condition is applied to the outlet of the column as it gives better convergence results and also prevents liquid entrainment with gas. At the outlet, pressure is specified to atmospheric pressure in all cases.

At $y = H$, $P = P_{atm}$

The walls are specified with a no-slip condition for the gas and liquid phases. Therefore, for a reactor of radius R, the following boundary condition is applied at the wall:

At $r = R$, $v_{y,g} = 0$ and $v_{y,l} = 0$

In order to get better picture of hydrodynamics, no symmetry conditions were used in the model. Since the effects of turbulence at the boundaries of liquid are difficult to approximate, iterations were used to specify the turbulent kinetic energy k and dissipation rate ε at the inlets and outlets.

3. Results
3. 1. Gas Holdup Versus Superficial Gas Velocity

The 3D CFD analysis of this paper is created using the software ANSYS FLUENT. The three-dimensional

curves of the gas holdup α_g in relation to the U_{gs} and the H are depicted in Figure 1. Figure 2 illustrates the impact of varying the U_{gs} (0.0283, 0.0567, 0.085 m/s) on the average gas holdup while varying the H (45, 55, 65cm) in an O_2-CuCl system. The contours of the cut sections of the BCR created in the centre of the XY and ZY planes are depicted in Figures 3-5. In order to facilitate a more comprehensive contour of α_g, additional cut sections have been created at heights of 10, 20, and 30 cm from the reactor's base on the ZX plane. The gas holdup's behaviour is strongly three-dimensional, as evidenced by the contours, which clearly indicate that it is not symmetrical on the XY, ZY, and ZX planes. The physical behaviour of α_g with U_{gs} is consistent with that of the Helium-Water system, as evidenced by the figures. Specifically, α_g increases as U_{gs} increases.
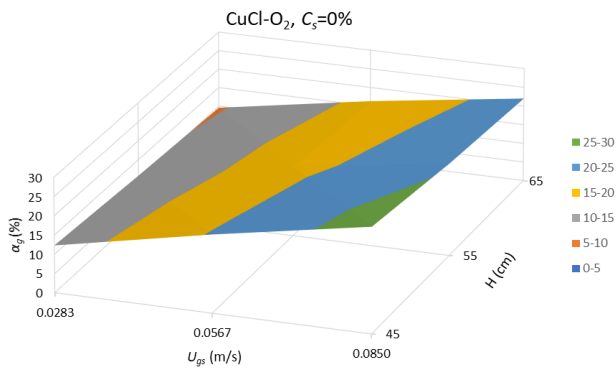

Fig. 1 Impact of superficial gas velocity and static liquid height on average gas holdup in the cucl-o2 system.
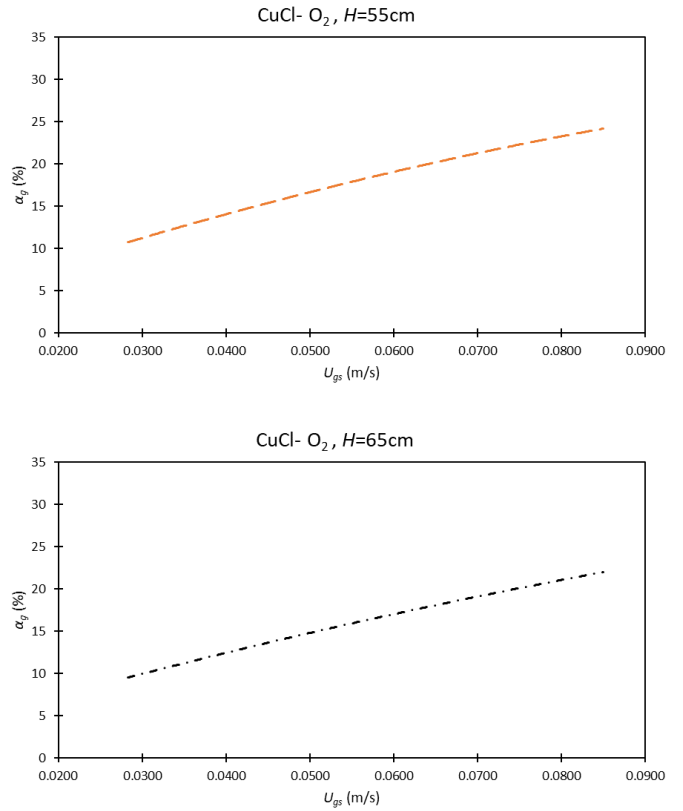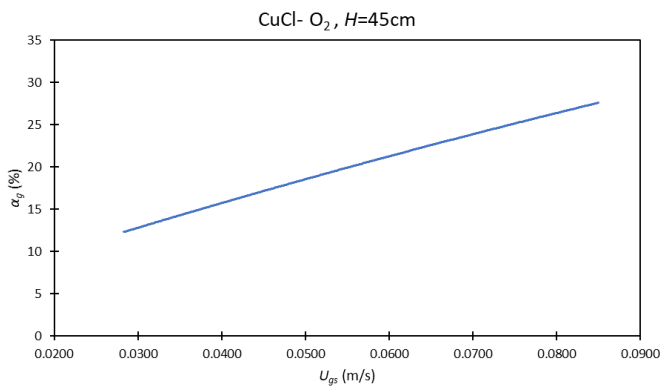

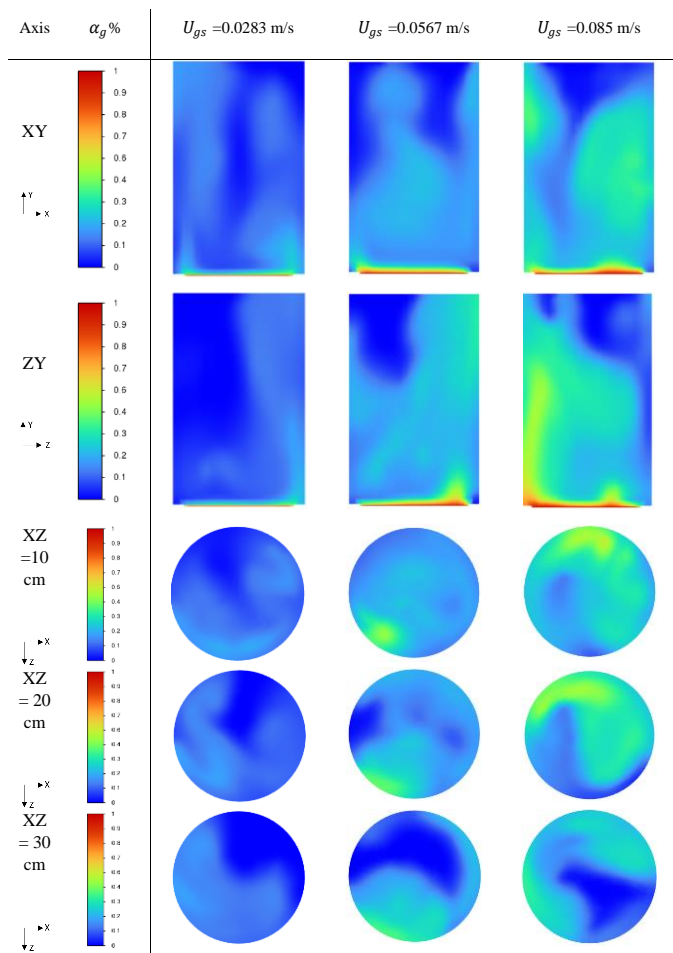Fig. 2 Relationship between average gas holdup and superficial gas velocity in the CuCl-O_2 system.

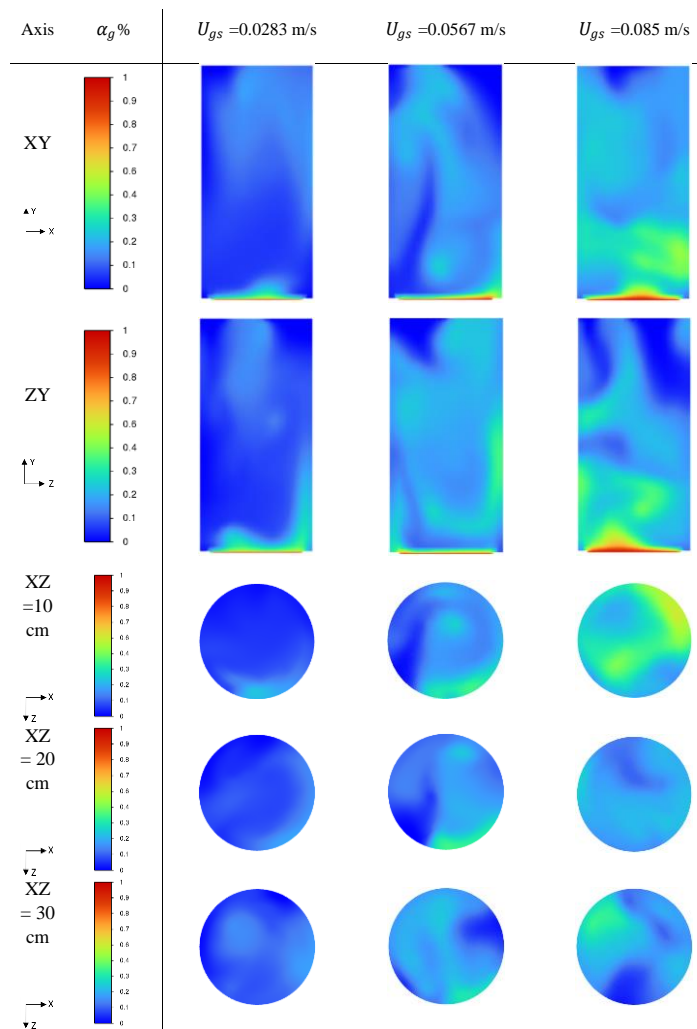Fig. 3 Gas holdup contours in Oxygen-CuCl system at H=45 cm.

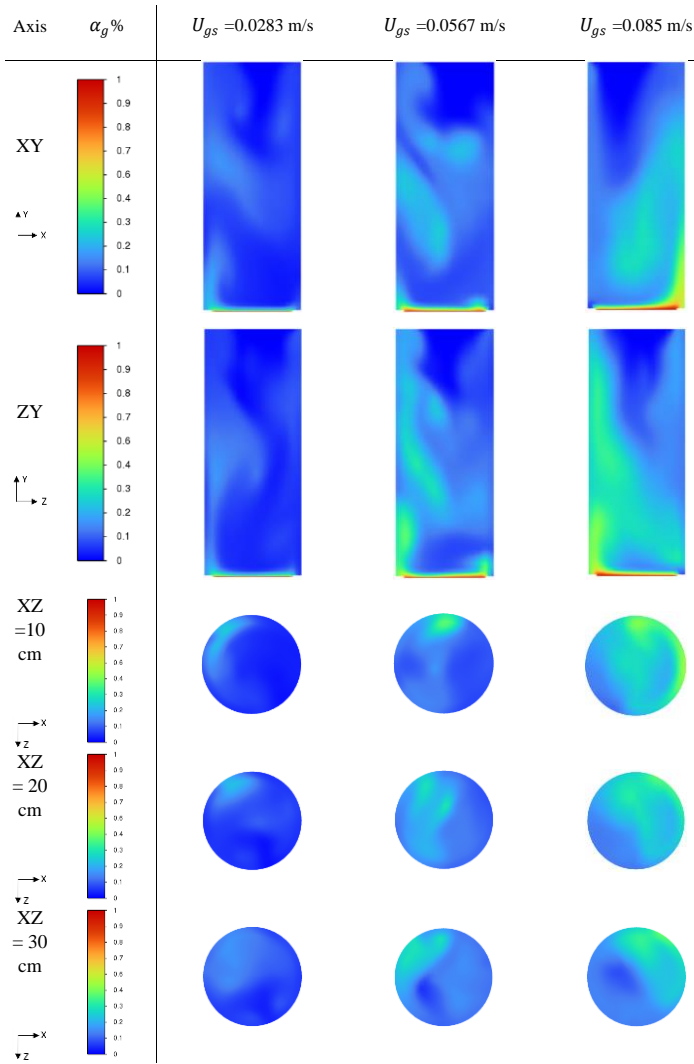Fig. 4 Gas holdup contours in Oxygen-CuCl system at H=55 cm.

Axis	$\alpha_g\%$	U_{gs} =0.0283 m/s	U_{gs} =0.0567 m/s	U_{gs} =0.085 m/s

Fig. 5 Gas holdup contours in Oxygen-CuCl system at H=65 cm.

3.2. 3D CFD Comparative Analysis of Water-Helium System vs CuCl-Oxygen System

The hydrodynamics dimensionless groups result of the actual materials (CuCl and O_2) and the simulated materials (He and H_2O) are compared in Table 2 according to the study of Abdulrahman [24-25]. The density ratio of gas to liquid, which is 11.311%, is the source of the maximum error in the dimensionless groups. The gas holdup values calculated for the actual and simulated materials are presented in Table 3, along with the percentage of errors generated by the discrepancy between the two. It is evident that the greatest percentage error is 29.9%. Additionally, it is evident that the gas holdup values in the actual materials are typically underestimated in comparison to those in the simulated materials. The superficial gas velocities of the actual materials were adjusted to produce analogous effects to those of the simulated materials. The high percent error can be attributed to the complexity of the multiphase system in 3D, as well as the accumulation of the percent errors generated from each of the hydrodynamic dimensionless parameters, as illustrated in Table 2. The trends and behaviour within the SBCR were effectively simulated by the 3D CuCl-O_2 simulation.

Table 2 Comparison of dimensionless groups in actual vs. experimental material percent error [24-25].

Dimensionless Group	Actual Material	Experimental Materials	Error %
$\dfrac{\rho_g}{\rho_l}$	0.000121	0.000135	11.311
$\dfrac{\mu_g}{\mu_l}$	0.021756	0.023	6.908
$\dfrac{Re_l^2}{We_l}$	76473868 (D_R=1m)	76085070 (D_R=1m)	0.508

Table 3 Comparative analysis of superficial gas velocity and gas holdup in water-helium and cucl-oxygen systems with error assessment at 45 cm static liquid height.

H_2O-He		CuCl-O_2		Error
U_{gs} (m/s)	α_g (%)	U_{gs} (m/s)	α_g (%)	(%)
0.05	16.0	0.0283	12.3	29.9
0.1	24.4	0.0576	20.4	19.6
0.15	31.3	0.085	27.6	13.3

In Fig. 4, it is evident that the gas holdup exhibits a similar behaviour in both the H_2-H_2O and O_2-CuCl systems. Specifically, the gas holdup increases as the superficial gas velocity increases and decreases as the static liquid height increases. The gas holdup values were more closely aggregated at various static liquid heights at lower velocities. Nevertheless, the gas holdup values were more dispersed at different heights as the superficial gas velocity increased.
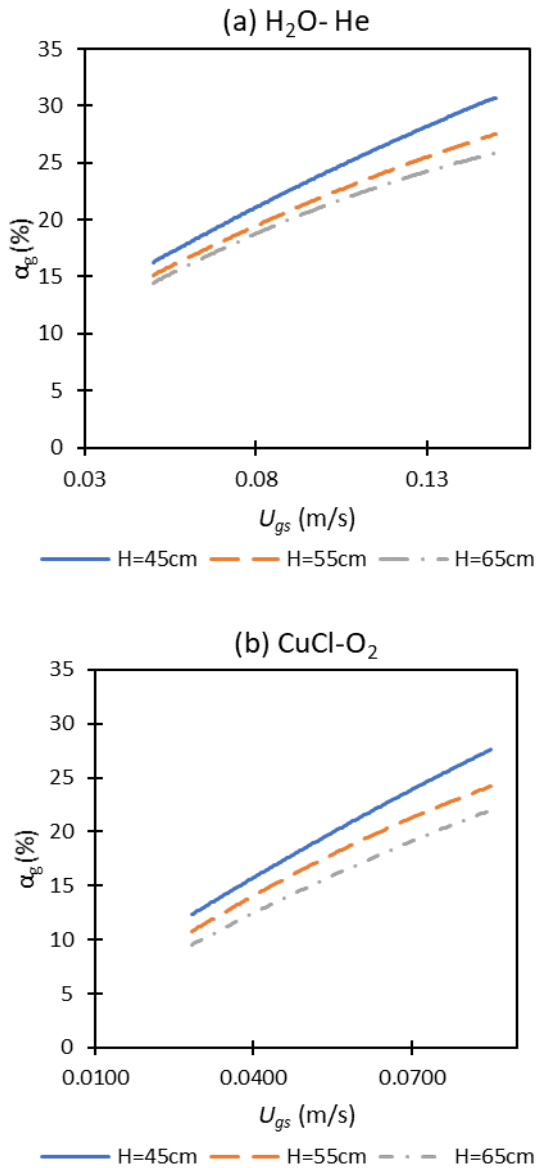
Fig.6 Comparative Study of Superficial Gas Velocity Effects on Gas Holdup at Varying Static Liquid Heights: (a) Water-Helium vs. (b) CuCl-Oxygen Systems.

5. Conclusions

The objective of this investigation is to verify the utilization of substitute materials, specifically liquid water and helium gas, in substitute of the actual materials, molten CuCl and oxygen gas, in the oxygen bubble column reactor for the thermochemical copper-chlorine (Cu-Cl) cycle of hydrogen production. The validation is conducted using 3D computational fluid dynamics (CFD) simulations with the ANSYS Fluent software, with a specific emphasis on the CuCl-O_2 system at varying superficial gas velocities. The patterns of gas

holdup as a function of superficial gas velocity are consistent across both 3D CFD simulations, as concluded. Additionally, the gas holdup in the 3D CFD results of the O_2-CuCl system is generally underestimated in comparison to the He-H_2O system.

List of Symbols

A_i	Interfacial area concentration
C	Specific heat
C_D	Drag coefficient
d_b	Bubble diameter
g	Gravitational acceleration
H	Height
Mi	Total interfacial forces between the phases
P	Phase pressure
$Q_{g,l}$	Heat exchange Intensity
Re	Reynolds number
T	Temperature
v	Velocity field
Vg	Volumes of gas
Vl	Volumes of liquid
U_{gs}	Superficial gas velocity
αg	Gas holdup
μ_{eff}	Effective viscosity
μ_g	Dynamic viscosity gas
μ_l	Dynamic viscosity liquid
ρ_g	Density, gas
ρ_l	Density, liquid
$\bar{\bar{\tau}}: \nabla V$	Viscous stress tensor

References

[1] Lewis, M. A., M. Serban, and J. K. Basco. "Generating hydrogen using a low temperature thermochemical cycle." In *Proceedings of the ANS/ENS 2003 Global International Conference on Nuclear Technology, New Orleans*. 2003.

[2] Serban, M., M. A. Lewis, and J. K. Basco. "Kinetic study of the hydrogen and oxygen production reactions in the copper-chloride thermochemical cycle." *AIChE 2004 spring national meeting, New Orleans, LA*. 2004.

[3] Abdulrahman, Mohammed W. "Similitude for Thermal Scale-up of a Multiphase Thermolysis Reactor in the Cu-Cl Cycle of a Hydrogen Production." *International Journal of Energy and Power Engineering,* vol. 10, no. 5, pp. 664-670, 2016.

[4] Abdulrahman, Mohammed W. "Heat Transfer Analysis of a Multiphase Oxygen Reactor Heated by

a Helical Tube in the Cu-Cl Cycle of a Hydrogen Production." *International Journal of Mechanical and Mechatronics Engineering,* vol. 10, no. 6, pp. 1122-1127, 2016.

[5] Abdulrahman, M. W., Wang, Z., Naterer, G. F., & Agelin-Chaab, M. "Thermohydraulics of a thermolysis reactor and heat exchangers in the Cu-Cl cycle of nuclear hydrogen production." In *Proceedings of the 5th World Hydrogen Technologies Convention,* 2013.

[6] Abdulrahman, Mohammed W. "Heat Transfer Analysis of the Spiral Baffled Jacketed Multiphase Oxygen Reactor in the Hydrogen Production Cu-Cl Cycle." In *Proceedings of the 9th International Conference on Fluid Flow, Heat and Mass Transfer (FFHMT'22)*, 2022.

[7] Abdulrahman, Mohammed W. "Review of the Thermal Hydraulics of Multi-Phase Oxygen Production Reactor in the Cu-Cl Cycle of Hydrogen Production." In *Proceedings of the 9th International Conference on Fluid Flow, Heat and Mass Transfer (FFHMT'22)*, 2022.

[8] Abdulrahman, Mohammed W. "Analysis of the thermal hydraulics of a multiphase oxygen production reactor in the Cu-Cl cycle." Diss. University of Ontario Institute of Technology (Canada), 2016.

[9] Ryskamp, J.M., Hildebrandt, P., Baba, O., Ballinger, R., Brodsky, R., Chi, H.W., Crutchfield, D., Estrada, H., Garnier, J.C., Gordon, G. and Hobbins, R. "*Design Features and Technology Uncertainties for the Next Generation Nuclear Plant.*" No. INEEL/EXT-04-01816. Idaho National Laboratory (INL), 2004.

[10] Shaikh, Ashfaq. *Bubble and slurry bubble column reactors: mixing, flow regime transition and scaleup*. Vol. 68. No. 09. 2007.

[11] Li, Z., Guan, X., Wang, L., Cheng, Y., & Li, X. "Experimental and numerical investigations of scale-up effects on the hydrodynamics of slurry bubble columns." *Chinese journal of chemical engineering*, vol. *24, no.* 8, pp. 963-971, 2016.

[12] Sarhan, A. R., Naser, J., & Brooks, G. "CFD modeling of bubble column: Influence of physico-chemical properties of the gas/liquid phases properties on bubble formation." *Separation and Purification Technology*, vol. 201, pp. 130-138, 2018.

[13] Li, Weiling, and Wenqi Zhong. "CFD Simulation of Hydrodynamics of Gas–Liquid–Solid Three-Phase Bubble Column." *Powder Technology*, vol. 286, pp. 766–788, 2015.

[14] Pu, W., Yang, N., Yue, C., Bai, S., & Chen, Y. "Simulation on direct contact heat transfer in gas-

molten salt bubble column for high temperature solar thermal storage." *International Communications in Heat and Mass Transfer*, vol. 104, pp. 51-59, 2019.

[15] Zhang, Xi-Bao, and Zheng-Hong Luo. "Local Gas–Liquid Slip Velocity Distribution in Bubble Columns and Its Relationship with Heat Transfer." *AIChE Journal*, vol. 67, no. 1, 2020.

[16] L Li, W Lian, B Bai, Y Zhao, P Li, Q Zhang, W Huang "CFD-PBM Investigation of the Hydrodynamics in a Slurry Bubble Column Reactor with a Circular Gas Distributor and Heat Exchanger Tube." *Chemical Engineering Science: X*, vol. 9 p. 100087, 2021.

[17] Zhou, Rongtao, Ning Yang, and Jinghai Li. "A conceptual model for analyzing particle effects on gas-liquid flows in slurry bubble columns." *Powder Technology,* vol. 365, pp. 28-38, 2020.

[18] Wodołażski, Artur. "CFD Hydrodynamics Analysis of Syngas Flow in Slurry Bubble Column." *Journal of Oil, Gas and Petrochemical Technology,* vol. 3, no.1, pp. 83-96, 2016.

[19] Matiazzo, T., Decker, R.K., Bastos, J.C.S.C., Silva, M.K. and Meier, H. "Investigation of Breakup and Coalescence Models for Churn-Turbulent Gas-Liquid Bubble Columns." *Journal of Applied Fluid Mechanics* vol. 13, no. 2, pp. 737-751, 2020.

[20] Ertekin, E., Kavanagh, J.M., Fletcher, D.F. and McClure, D.D. "Validation studies to assist in the development of scale and system independent CFD models for industrial bubble columns." *Chemical Engineering Research and Design*, vol. 171, pp. 1-12, 2021.

[21] Yan, P., Jin, H., He, G., Guo, X., Ma, L., Yang, S. and Zhang, R. "CFD simulation of hydrodynamics in a high-pressure bubble column using three optimized drag models of bubble swarm." *Chemical Engineering Science*, vol. 199, pp. 137-155, 2019.

[22] Adam, Salman, and Kalthoum Tuwaechi. "Hydraulic Simulation of Bubble Flow in Bubble Column Reactor." *Journal of Complex Flow*, vol. 1, no. 2, 2019.

[23] Pourtousi, M., P. Ganesan, and J. N. Sahu. "Effect of bubble diameter size on prediction of flow pattern in Euler–Euler simulation of homogeneous bubble column regime." *Measurement*, vol. 76, pp. 255-270, 2015.

[24] Abdulrahman, Mohammed Wassef. "Material substitution of cuprous chloride molten salt and oxygen gas in the thermolysis reactor of hydrogen production Cu—Cl cycle." U.S. Patent No. 10,526,201. 7 Jan. 2020.

[25] Abdulrahman, Mohammed W. "Simulation of Materials Used in the Multiphase Oxygen Reactor of Hydrogen Production Cu-Cl Cycle." In *Proceedings of the 6 the International Conference of Fluid Flow, Heat and Mass Transfer (FFHMT'19)*. 2019.

[26] Abdulrahman, M. W. "Experimental studies of gas holdup in a slurry bubble column at high gas temperature of a helium− water− alumina system." *Chemical Engineering Research and Design*, vol. 109, pp. 486-494, 2016.

[27] Abdulrahman, M. W. "Experimental studies of the transition velocity in a slurry bubble column at high gas temperature of a helium–water–alumina system." *Experimental Thermal and Fluid Science*, vol. 74, pp. 404-410, 2016.

[28] Abdulrahman, M. W. "Experimental studies of direct contact heat transfer in a slurry bubble column at high gas temperature of a helium–water–alumina system." *Applied Thermal Engineering*, vol. 91, pp. 515-524, 2015.

[29] Abdulrahman, Mohammed Wassef. "Direct contact heat transfer in the thermolysis reactor of hydrogen production Cu—Cl cycle." U.S. Patent No. 10,059,586. 28 Aug. 2018.

[30] Abdulrahman, M. W., Wang, Z. & Naterer, G. F. "Thermohydraulics of a thermolysis reactor and heat exchangers in the Cu-Cl cycle of nuclear hydrogen production." In *Proceedings of the 5th World Hydrogen Technologies Convention*, 2013.

[31] Abdulrahman, Mohammed W. "CFD Simulations of Gas Holdup in a Bubble Column at High Gas Temperature of a Helium-Water System." In *Proceedings of the 7th World Congress on Mechanical, Chemical, and Material Engineering (MCM'20)*, 2020

[32] Abdulrahman, M.W. "CFD Simulations of Direct Contact Volumetric Heat Transfer Coefficient in a Slurry Bubble Column at a High Gas Temperature of a Helium–Water–Alumina System." *Applied Thermal Engineering*, vol. 99, pp. 224–234, 2016.

[33] Abdulrahman, Mohammed W. "CFD Analysis of Temperature Distributions in a Slurry Bubble Column with Direct Contact Heat Transfer." In *Proceedings of the 3rd International Conference on Fluid Flow, Heat and Mass Transfer (FFHMT'16)*. 2016.

[34] Abdulrahman, Mohammed W. "Temperature profiles of a direct contact heat transfer in a slurry bubble column." *Chemical Engineering Research and Design*, vol. 182, pp. 183-193, 2022.

[35] Abdulrahman, Mohammed W. "Effect of Solid Particles on Gas Holdup in a Slurry Bubble Column." In *Proceedings of the 6th World Congress on Mechanical, Chemical, and Material Engineering*, 2020.

[36] Abdulrahman, Mohammed W., and Nibras Nassar. "Eulerian Approach to CFD Analysis of a Bubble Column Reactor–A." In *Proceedings of the 8th World Congress on Mechanical, Chemical, and Material Engineering (MCM'22)*, 2022.

[37] Abdulrahman, M. W., & Nassar, N. "Three Dimensional CFD Analyses for the Effect of Solid Concentration on Gas Holdup in a Slurry Bubble Column." In *Proceedings of the 9th World Congress on Mechanical, Chemical, and Material Engineering (MCM'23)*, 2023.

[38] Abdulrahman, M. W., & Nassar, N. "Effect of static liquid height on gas holdup of a bubble column reactor." In *Proceedings of the 9th World Congress on Mechanical, Chemical, and Material Engineering (MCM'23)*, 2023.

[39] Abdulrahman, M. W., & Nassar, N. "A three-dimensional CFD analyses for the gas holdup in a bubble column reactor." In *Proceedings of the 9th World Congress on Mechanical, Chemical, and Material Engineering (MCM'23)*, 2023.

[40] Nassar, Nibras Ibrahim, "A Three-Dimensional CFD Analysis for the Hydrodynamics of the Direct Contact Heat Transfer in the Oxygen Production Slurry Bubble Column Reactor of the CU-CL Cycle of Hydrogen Production." Thesis. Rochester Institute of Technology, 2023.

[41] Abdulrahman, M. W., & Nassar, N. "Hydrodynamic Analysis of Oxygen and Molten CuCl in the Cu-Cl Cycle Using a 3D CFD Model for Hydrogen Production" In *Proceedings of the 10th World Congress on Mechanical, Chemical, and Material Engineering (MCM'24)*, 2024.

[42] Abdulrahman, M. W., & Nassar, N. "Impact of Static Liquid Height on Hydrodynamics of the Thermolysis Reactor in the Cu-Cl Cycle for Hydrogen Production" In *Proceedings of the 10th World Congress on Mechanical, Chemical, and Material Engineering (MCM'24)*, 2024.

[43] *ANSYS FLUENT Theory Guide*, Release 14.5. ANSYS, Inc., 2012.

[44] L. Schiller, A. Naumann, Uber die grundlegenden berechnungen bei der schwerkraftaufbereitung / About the basic calculations in the gravity-treatment, Zeitung des vereins deutscher ingenieure / Newspaper of the Association of German Engineers, pp. 77–318, 1933.